IS-T 1770

A New Post-column Reactor-laser Induced Fluorescence Detector for Capillary Electrophoresis

by

Zhang, Liling

MS Thesis submitted to Iowa State University

Ames Laboratory, U.S. DOE

Iowa State University

Ames, Iowa 50011

Date Transmitted: January 2, 1996

PREPARED FOR THE U.S. DEPARTMENT OF ENERGY

UNDER CONTRACT NO. W-7405-Eng-82.

DISCLAIMER

TABLE OF CONTENTS

CHAPTER 1
GENERAL INTRODUCTION

Capillary Zone Electrophoresis. Capillary zone electrophoresis (CZE), a powerful separation method based on the differential migration of charged species under the influence of an electric field, has been widely used for separations covering from small ions [1,2] to big biomolecules [3-5].

The basic instrumentation of a CZE system, shown in Fig. 1, consists of a high power supply, a narrow bore fused silica capillary filled with an electrolyte solution (buffer), two electrolyte reservoirs in connection with the power supply via metal electrodes, a detector, and a data collecting device.

Upon application of a potential to a bare silica capillary, there are two flow phenomena in the capillary, as shown in Fig. 2. The movement of the uncharged liquid relative to the capillary wall is known as the electroosmotic flow (EOF). The EOF originates from an electric double layer between the charged inner surface of the capillary and counter ions in the electrolyte solution. Silanol groups (pKa < 2) on the capillary wall could exist as $SiOH^+$, SiOH, or SiO^- depending on the pH of the electrolyte solution. The electric double layer can be viewed by Stern's double layer model, which states that the double layer consists of a compact layer and a diffuse layer. In the compact layer, counter ions tend to adsorbed onto the capillary wall with a mono-molecular thickness. In the diffuse layer, counter ions have freedom to move around and the movement is governed by thermal motion. Under the influence of an applied potential, a portion of the diffuse layer moves resulting in the electroosmotic flow. The diffuse layer thickness, β(cm), can be estimated as follows[6]:

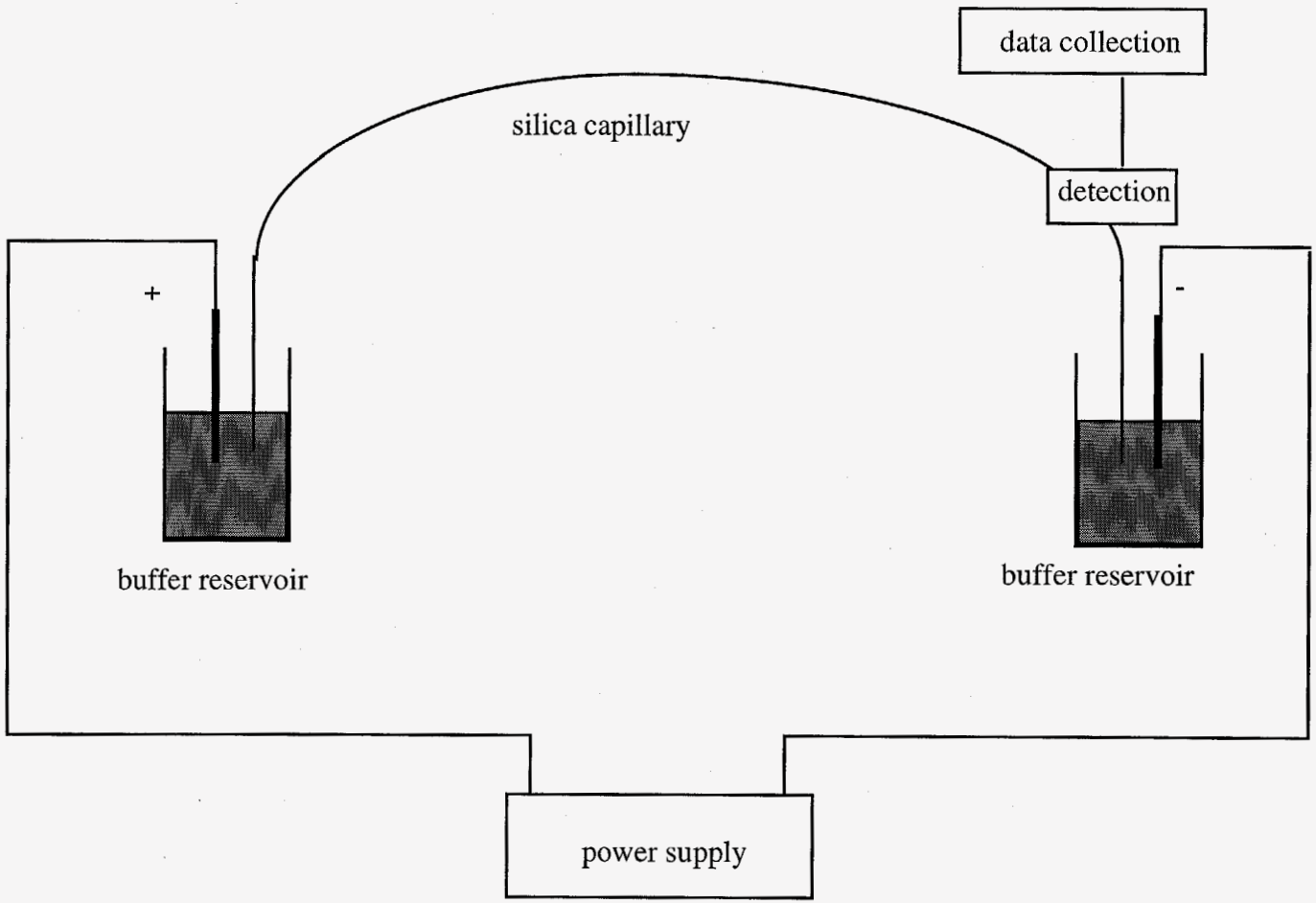

Figure 1. A Capillary Electrophoresis System.

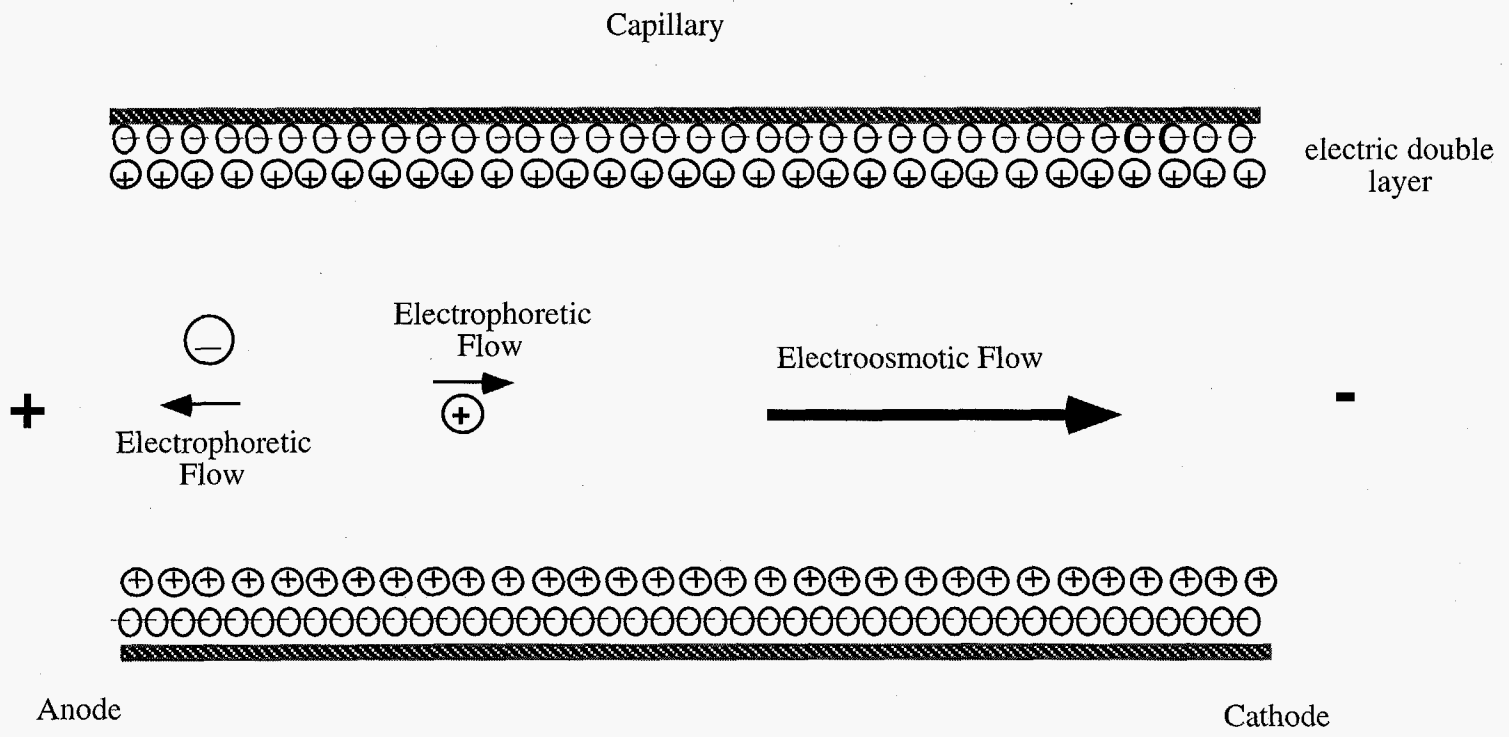

Figure 2. The Electroosmotic Flow and The Electrophoretic Flow.

$$\beta = \frac{3\times10^{-8}}{\sqrt{I}} \quad (1)$$

where I is the ionic strength of the buffer .

Within the compact layer, the potential drops linearly with the distance from the surface, x, while in the diffuse layer the potential, known as the zeta potential, ζ, drops exponentially with x.

The velocity of the EOF, v_{eo} (cm/s) is described as [6]:

$$v_{eo} = \frac{\xi\varepsilon}{4\pi\eta}E = \mu_{eo}E \quad (2)$$

where E is the applied electric field (V/cm), ζ is the zeta potential (V), ε is the dielectric constant of the medium(F/m), η is the viscosity of the solution(Pa · s) and μ_{eo} is the electroosmotic mobility ($cm^2/V{\cdot}s$).

As seen in equation (2), the electroosmotic mobility is directly proportional to the zeta potential. The pH value and the ionic strength of the buffer are two major factors influencing the zeta potential. High pH values cause more dissociation of surface silanols leading to an increased zeta potential. However, at pH > 8, silanols are completely dissociated and further increasing pH has no effect on the zeta potential. The zeta potential drops at high ionic strength, because the diffusion layer thickness decreases.

Unlike the parabolic flow profile in any pressure-driven system such as HPLC, CZE, being an electrically-driven system, has a uniform EOF velocity across the capillary giving rise to a plug-like flow profile, as shown in Fig. 3. Band broadening from the parabolic flow is negligible in CZE, and this is one of the major reasons that CZE has higher separation efficiencies than HPLC. In most cases, the capillary inner wall is negatively charged, and the solution side of the electric double larger has cations as counter ions. Therefore, the EOF goes

Pressure Flow: Parabolic Velocity Profile

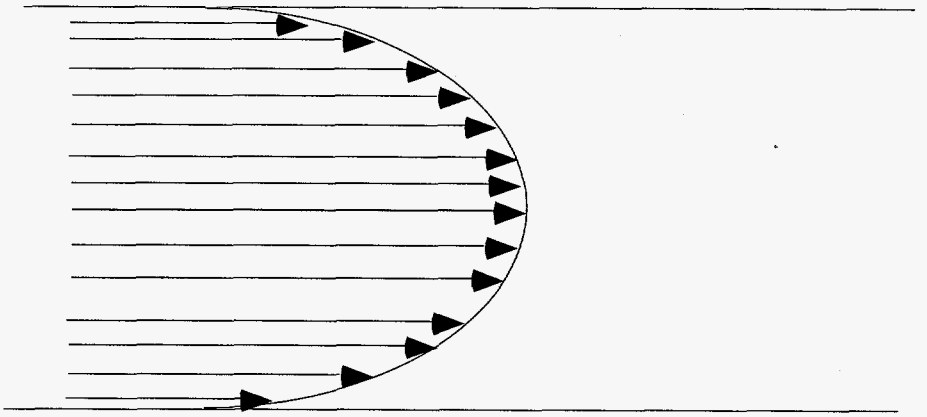

Electroosmotic Flow: Flat Velocity Profile

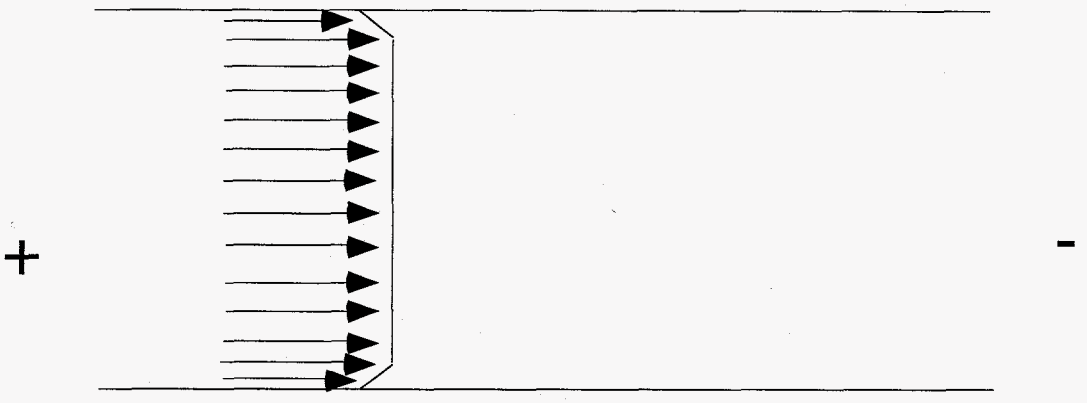

Figure 3. The Flow Profile of A Pressure and An Electroosmotic Flow.

from the anode to the cathode. The magnitude of the EOF is usually strong enough to carry all the species from the anode to the cathode, regardless of their charges. This is fortunate since anions and cations can be separated and detected at the same time. The EOF, however, does not contribute to the separation because it carries all the sample components along the capillary at the same speed. The differential migration comes solely from electrophoretic migrations of ionic species, or electrophoretic flow (EPF), which is the motion of charged species under the influence of an applied potential.

The velocity of the EPF, v (cm/s) can be calculated by [6]:

$$v = \frac{z_i e_o}{6\pi\eta r_i} E = \mu_e E \qquad (3)$$

where z_i is the charge number of species i, e_o is the elemental charge, r_i is the radius of the solvated ion (cm), and μ_e is the electrophoretic mobility ($cm^2/V \cdot s$). Species with different charge-to-size ratio migrate along the capillary at different electrophoretic velocities, which results in separations.

The separation process is initiated by applying an electric field after the sample injection. Sample introduction in CZE can be either done hydrodynamically or electrokinetically. The electrokinetic injection may result in chemical discrimination, and therefore, the hydrodynamic injection is usually preferred.

The separation efficiency in CZE is measured by the theoretical plate number, N, as in chromatography. N can be calculated as [6]:

$$N = \frac{(\mu + \mu_{eo})}{2D} V \qquad (4)$$

where D is the diffusion coefficient (cm^2/s), V is the applied potential (V). Equation (4) shows that N is directly proportional to the applied potential, which suggests the high

efficiency with high potential. In practice, however, use of very high potential may deteriorate the efficiency due to additional band broadening from Joule heating. A high electroosmotic mobility from a high field strength transports analyte zones rapidly through the capillary. There are two consequences from the rapid transportation. One is the sharp zone due to little time for diffusion to broaden the analyte zones, which is translated into high separation efficiencies. The other consequence is poor resolution due to little time for neighboring zones to be resolved by differential electromigration.

The resolution of two peaks, R, in CZE can be calculated as [6]:

$$R = 0.177(\mu_1 - \mu_2)\sqrt{\frac{V}{D(\bar{\mu} + \mu_{eo})}} \qquad (5)$$

where μ_1 and μ_2 are electrophoretic mobilities of component 1 and 2, respectively. V is the applied potential across the capillary and $\bar{\mu}$ is the mean electrophoretic mobility.

High resolutions can be obtained by adjusting the EOF so that it moves against the EPF, or by suppressing the EOF with surface coating [7]. The trade off of the high resolution separations is the long separation times.

Assuming Gaussian peak shapes, the band width can be expressed by the variance, σ^2, and the total variance, σ_t^2, is the sum of variances from all sources of band broadening, which includes the axial diffusion, σ_D^2, adsorption, σ_A^2, Joule heating, σ_J^2, electrophoretic dispersion, σ_E^2, injection, σ_I^2 , and detection, σ_W^2 , [6]:

$$\sigma_t^2 = \sigma_D^2 + \sigma_A^2 + \sigma_J^2 + \sigma_E^2 + \sigma_I^2 + \sigma_W^2 \qquad (6)$$

Axial diffusion, driven by a concentration gradient, can never be totally eliminated. σ_D^2 relates to the diffusion coefficient as follows [6]:

$$\sigma_D^2 = 2Dt \qquad (7)$$

where t is the migrating time (s) from the injection end to the detector.

Adsorption of sample constituents to the capillary wall results in tailing, and it is more pronounced for small i. d. capillaries [8]. Surface coating is an effective method to reduce the adverse effect of the adsorption [7]. Adsorption can also be simply reduced by coulombic repulsion if the analyte ions can bare the same charge sign as the capillary wall through adjusting of the buffer pH.

Joule heating, coming from conversion of electricity energy to heat, occurs whenever a current passes a capillary. Heat is generated homogeneously across the capillary bore and dissipates through the capillary wall. As a result, a parabolic temperature profile is formed. The parabolic temperature profile gives rise to a parabolic migration velocity profile since viscosity has a dependence on the temperature. Joule heating can seriously degrade the efficiency.

The rate of heat generated per unit volume, Q, (w/cm^{-3}) is [6]:

$$Q = E^2 \Lambda C \phi \qquad (8)$$

Where Λ is the equivalence conductance of the buffer (cm2/Ω.mol), C is the molar concentration of the buffer (M) and ϕ is the total porosity of the medium and E is the field strength (V/cm).

The use of narrow bore capillaries, which generates less heat and dissipates more effectively than the wide bore capillary, low conductance and low molar concentration buffers help reducing band broadening from Joule heating.

Electrophoretic dispersion, originating from the difference in mobilities between sample ions and the buffer coion (the buffer ion baring the same charge sign as the sample ions), leads

to asymmetric peak shapes. Electrophoretic dispersion does not broaden zones significantly when the buffer concentration is at least 100 times greater the sample concentration. Under these conditions, the conductivity is primarily determined by the buffer.

The variance due to injection is [6]:

$$\sigma_I^2 = \frac{l^2}{12} \tag{9}$$

where l is the width of the initial sample pulse (cm).

σ_I^2 can be controlled by injection time, injection voltage (electrokinetic injection) or the sampling height (hydrodynamic injection).

Detection in Capillary Zone Electrophoresis. In CZE, separated analytes can be detected optically [9], electrochemically [10,11] or mass spectrometrically [12]. Small volume detector cell is very important in designing CZE detectors since a typical analyte zone is on the order of nanoliters [9]. To preserve the separation efficiency, the detector volume should be less than 10% of the peak volume. The maximum allowable detector dead volume v (nanoliter) is given by [9]:

$$v = \frac{100\pi d^2 L}{\sqrt{N}} \tag{10}$$

where d is the inner diameter of a capillary (μm), L is the capillary length to the detector (mm), and N is the theoretical plate number.

Other than small cell volume, a good CZE detector should also provide a high sensitivity, large dynamic range, and fast response.

Laser Induced Fluorescence (LIF) Detection in CZE. Among all detection modes, laser induced fluorescence (LIF), with mass limits of detection as low as 10^{-21} mol [13], represents the most promising method to meet the detection challenge posed by intrinsic small injection volumes in CE (subnanoliters). The very high sensitivity of LIF comes from low background, the high light intensity and efficient light coupling to the capillary core [9]. Laser induced native fluorescence has been shown to be very sensitive to tryptophan- and tyrosine-containing proteins and catecholamines [14-16]. A limit of detection of 1×10^{-10} M for conalbumin has been achieved using the 275.4-nm line from an argon-ion laser[14], and subsequently, hemoglobin and carbonic anhydrase were quantified on a cell-by-cell basis in human erythrocytes [15]. Limits of detection of catecholamines are in the nanomolar range with the same detection scheme as that in Ref. 14, and epinephrine along with norepinephrine were quantified in individual adrenal medullary cells [16].

Chemical Derivatization for Detection. When fluorescence detection is incorporated into non-fluorescing analytes, chemical derivatization, usually providing better detection sensitivity, must be implemented either before or after a separation. Pre-column derivatization, in which chemical reactions are performed before separations, has less restraints on chemical reactions. The derivatives, however, should be reasonably stable. Reactions, having slow kinetics, needing extreme conditions such as high temperature, fit well in a pre-column scheme. Also, excess derivatization reagent can be removed before injection to eliminate potential interference. On-line dilution and inefficient mixing are not of a concern. From the point view of instrumentation, pre-column mode is relatively straight forward since it does not need a reactor. However, a single analyte may give multiple peaks if it has different labeling sites[17], and separations of derivatives may be difficult because they may become alike after derivatization. Fluorescein isothiocyanate derivatized amino acids need micelle to be adequately separated[18].

Pre-column has been shown to be a very sensitive technique. Amino acids in individual snail neutron cells were derivatized with naphthalene-2,3-dicarboxaldehyde and cyanide (NDA/CN^-). The derivatives were detected amperometrically[19]. The total volume after the derivatiztion was only 25 nL which was not easy to handle. One way to avoid handling very small volumes is to carry reactions on column[20]. Individual rat pherochromocytoma cells were injected into the starting end of a capillary, and then lysed on column. Amino acids in the cells were derivatized with NDA/CN^-, separated by CE and detected by LIF. On-column preconcentration of derivatized sample zones before separation has also been incorporated in a pre-column derivztization scheme for better sensitivities[21].

Post-column derivatization is an alternative for pre-column derivatization. Ideally, post-column labeling reagent reacts rapidly with the analytes and itself does not interfere with the detection. Unstable derivatives may be useful in a post-column mode. Since reactions are performed on-column, subnanoliter sample volumes can be easily handled with a post-column reactor. Good post-column reactors provide efficient mixing to ensure rapid and complete reactions, and have small dead volumes so that minimal band broadening and dilution are resulted.

Several post-column reactors have been constructed for CE. In coaxial reactors[22-24], a separation capillary was inserted in a reaction capillary and the junction was held in a tee. Reaction reagents, driven by pressure, were introduced through the third arm of the tee. A low dead volume cross type connector was fabricated on a capillary by drilling holes into the capillary[25]. Reaction reagents have also been introduced into a gap between two closed aligned capillaries (several micrometers apart). Two capillaries with different inner diameters[26], or with the same inner diameters[27] have been used in the gap type reactors. A post-column reaction has been carried out in the terminal buffer reservoir containing reaction the reagent and derivatives were detected near the capillary tip[27]. A post-column reactor has also been fabricated on a glass microchip, an example of instrumentation miniaturization[28].

O-Phthaldialdehyde as the Post-Column Reagent. As shown in Fig. 4, *O*-phthaldialdehyde (OPA) reacts with primary amines at alkaline pH and room temperature in the presence of 2-mercaptoethyanol (2-ME) to give fluorescent derivatives with maximum excitation and emission at 340nm and 455 nm, respectively [29,30]. The reaction is usually carried in a borate buffer and completes within one minute[31]. The product, identified as an isoindole[30], is not stable. An intramolecular rearrangement through a nucleophilic attack by the ME oxygen was considered as one source contributing to the decomposition of the fluorescent product[32].

OPA derivatives of amino acids have similar quantum yields ranging from 0.33 to 0.47. OPA is less efficient with peptides, with quantum yields as low as 0.03, owing to the quenching of the isoindole fluorescence by the carboxyamide group[33].

Being a non-fluorescent and rapid reacting reagent, OPA has been widely used as a post-column reagent in both HPLC [34,35] and CZE[22, 25, 27, 28].

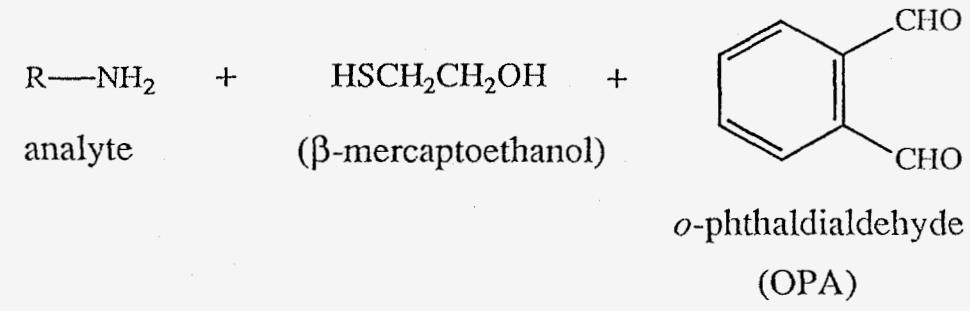

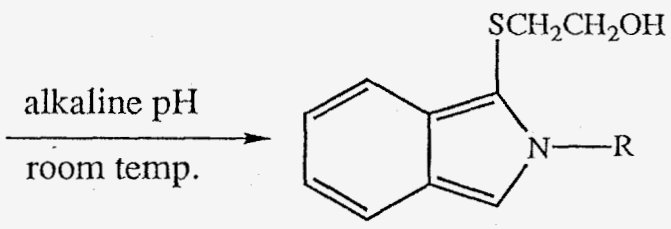

isoindole λ_{ex}= 340 nm
λ_{em}= 455 nm

CHAPTER 2

THE NEW POST-COLUMN REACTOR

This thesis describes a post-column reactor using two narrow bore capillaries connected coaxially. This reactor differs from other coaxial reactors in terms of capillary dimensions, reagent flow control, ease of construction and most importantly, better limits of detection. The use of 15-μm i.d. vs. 25-50-μm i.d. capillaries reduces on-column dilution making the reactor amenable to single cell analysis, which has been a very active research field in CE [36]. The derivatization reagent is electroosmotically driven into the reaction capillary and the reagent flow rate is independently controlled by a high voltage power supply. Amino acid, amines and proteins, derivatized OPA/2-ME using this post-column reactor coupled with LIF detection, show low attomole mass limits of detection, and for the first time, we demonstrate single cell (single human erythrocytes) capability with a post-column derivatization scheme.

Post-Column Reactor. Fig.5 shows a cross section of the post-column reactor consisting of two capillaries (Polymicro Technologies, Phoenix, AZ, USA). A 2-cm section of polyimide coating was burnt off from one end of a 15-μm i.d.x 150-μm o.d. capillary, which functioned as the separation capillary, and this end of the capillary was etched in a concentrated hydrofluoric acid solution (Aldrich Chemical Co., Milwaukee, WI, USA) until the outer diameter was smaller than 30- μm. The etched section was then dipped briefly in a saturated sodium carbonate solution and rinsed with deionized water. A 1-cm section from the etched tip was cut off because the inner walls near the tip were also etched by hydrofluoric acid drawn into the capillary by the capillary force. The rest of the etched section was carefully inserted

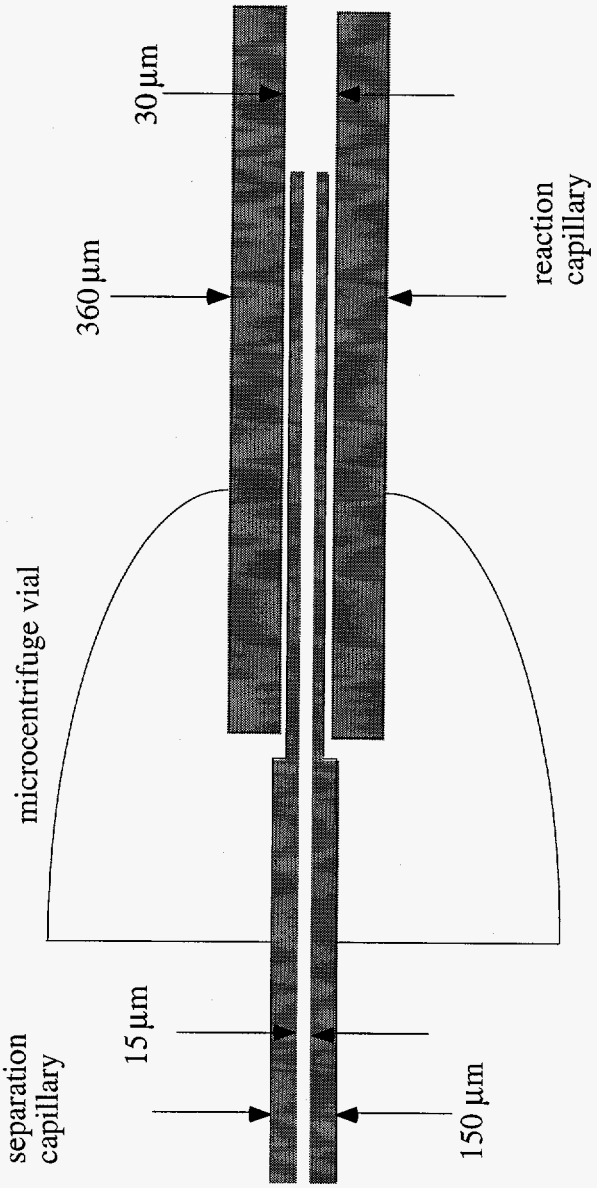

Figure 5. A Schematic Diagram of the Post-Column Reactor.

into a 30-μm i.d. x 360-μm o.d. capillary, which functioned as the reaction column. The junction was carefully slid into a micro centrifuge vial (Midwest Scientific, St. Louis, MO, USA) through two small holes drilled through the cap and the bottom of the vial in which the derivatization reagent was held during experiments. Capillaries were secured onto the vial with 5 Minute Epoxy (True Value Hardware Stores, Chicago, IL, USA).

Some preliminary tests were performed with reactors made from 50-μm i. d. x 150-μm i.d. and 150-μm i.d. x 360-μm o.d. capillaries. These reactors were put together by removal of 1-cm polyimide coating of a 50-μm i.d. capillary and insertion of this section into a 150-μm i.d. capillary without any chemical etching.

Instrumentation. The CE apparatus coupled with a LIF detection system, shown in Fig. 6, is home built. A 30 kV d.c. power supply (Glassman High Voltages, Whitehorse Station, NJ, USA) was connected between the inlet of the separation capillary and the micro centrifuge vial, which was grounded, while a 3 kV d.c. power supply (Bertan, Hicksville, NY, USA) was connected between the ground and the outlet of the reaction capillary. A glass microscope slide, onto which the post-column assembly was glued with 5 Minute Epoxy, was mounted to a two-dimensional stage (Edmund Scientific, Barrington, NJ, USA)with an angle about 110° relative to a 325-nm incident laser beam from a HeCd laser (Model 4240PS; Liconix, Sunnyvale, CA, USA). As depicted in Fig. 7, the incident beam was focused by a 1-cm focal length glass lens (Edmund Scientific) and the fluorescence emission was focused by a 20x microscope objective (Edmund Scientific) onto a R928 photomultiplier tube (PMT) (Hamamatsu, Bridgewater, NJ, USA). A 456-nm interference filter was placed in front of the PMT which was biased at -950 volts. Fluorescence signals were converted into voltages through a 10-kW resister. Data was collected via a 24-bit A/D interface (Justice Innovation, Palo Alto, CA, USA) at 5 Hz and stored in an IBM PC/AT 286 computer (IBM, Boca Raton,

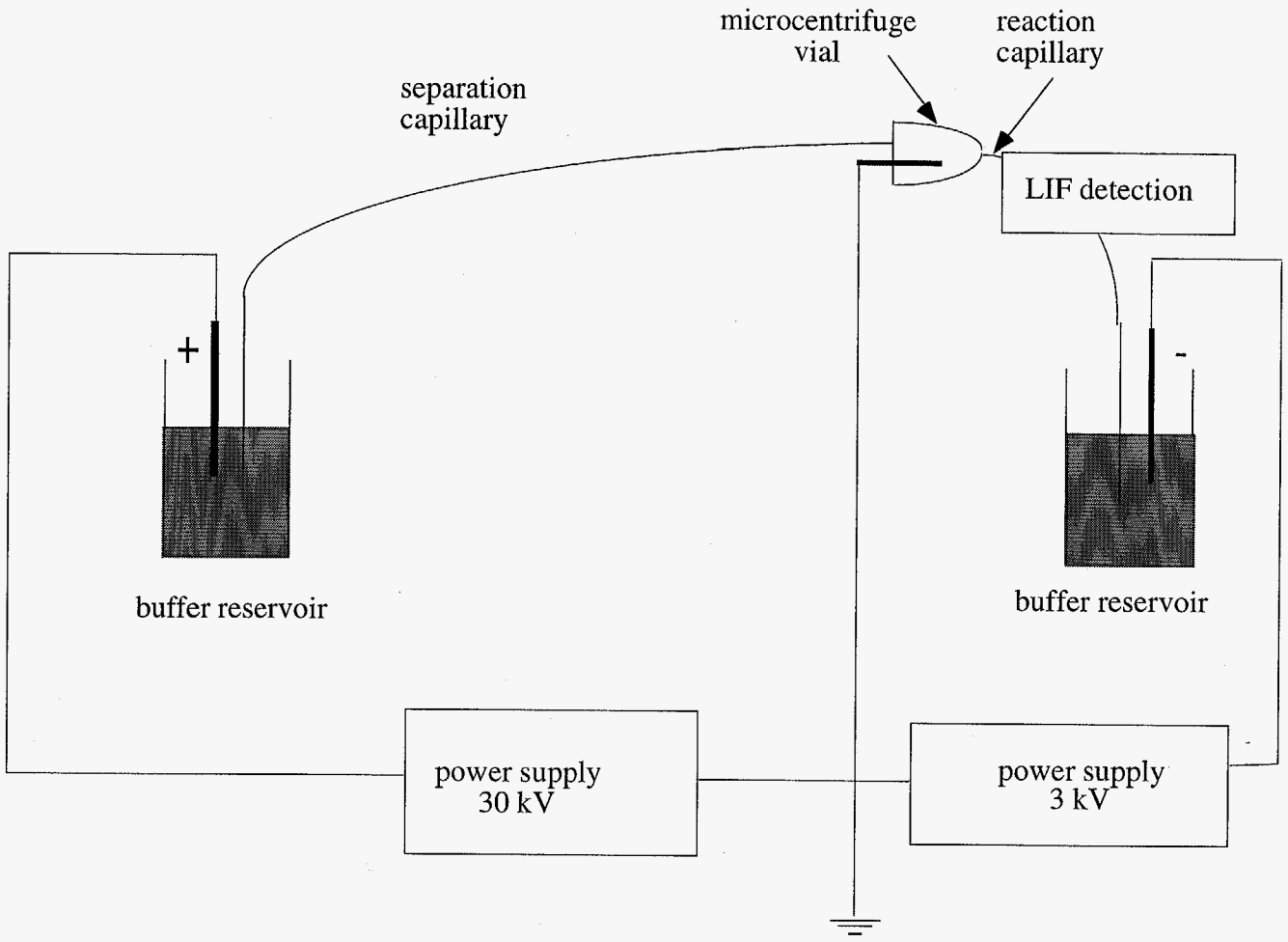

Figure 6. The Capillary Electrophoresis Coupled with Post-Column Reactor and Laser Induced Fluorescence Detection.

FL, USA). The entire electrophoresis and detection system were enclosed in a sheet-metal box with a high voltage interlock.

Samples were introduced by electrokinetic injections, and derivatives were detected at about 5mm from the outlet of the separation capillary. New reactors were pressure flushed with 1 M NaOH for 30 minutes followed by a 5 minute rinse with deionized water, and then equilibrated with running buffer under low field strength overnight.

Reagents and Samples. All chemicals were purchased from Sigma (St. Louis, MO, USA) unless otherwise noted. Fluorescein was from Molecular Probes (Eugene OR, USA). Water used for solution preparation was from a Milli-Q system (Millipore, Bedford, MA, USA). Borate buffer, used for all experiments, was made by adjusting a sodium tetraborate solution (20 mM) to pH 9.5 with NaOH. Samples were prepared in the borate buffer.The OPA reagent was made by dissolving 2 mg of *o*-phthaldialdehyde in a mixture of 3.9-mL borate buffer, 80-mL ethanol and 20-mL 2-mercaptoethanol. The reagent was aged overnight at 4 °C and discarded after 48 hours. Prior to use, buffer, sample and OPA solutions were filtered with 0.2 mm filters (Alltech, Deerfield, IL, USA).

Human erythrocytes were isolated by washing whole blood samples with a phosphate buffer saline solution (135 mM NaCl and 20 mM NaH_2PO_4 at pH 7.4) as described before[15]. The washed cells were suspended in an 8% glucose solution before injection and stored at 4 °C when not used. Fig 8. shows the single cell injection. Cells were introduced into the separation capillary by gentle suction from the outlet end of the reaction capillary placed in an air tight vial [15].

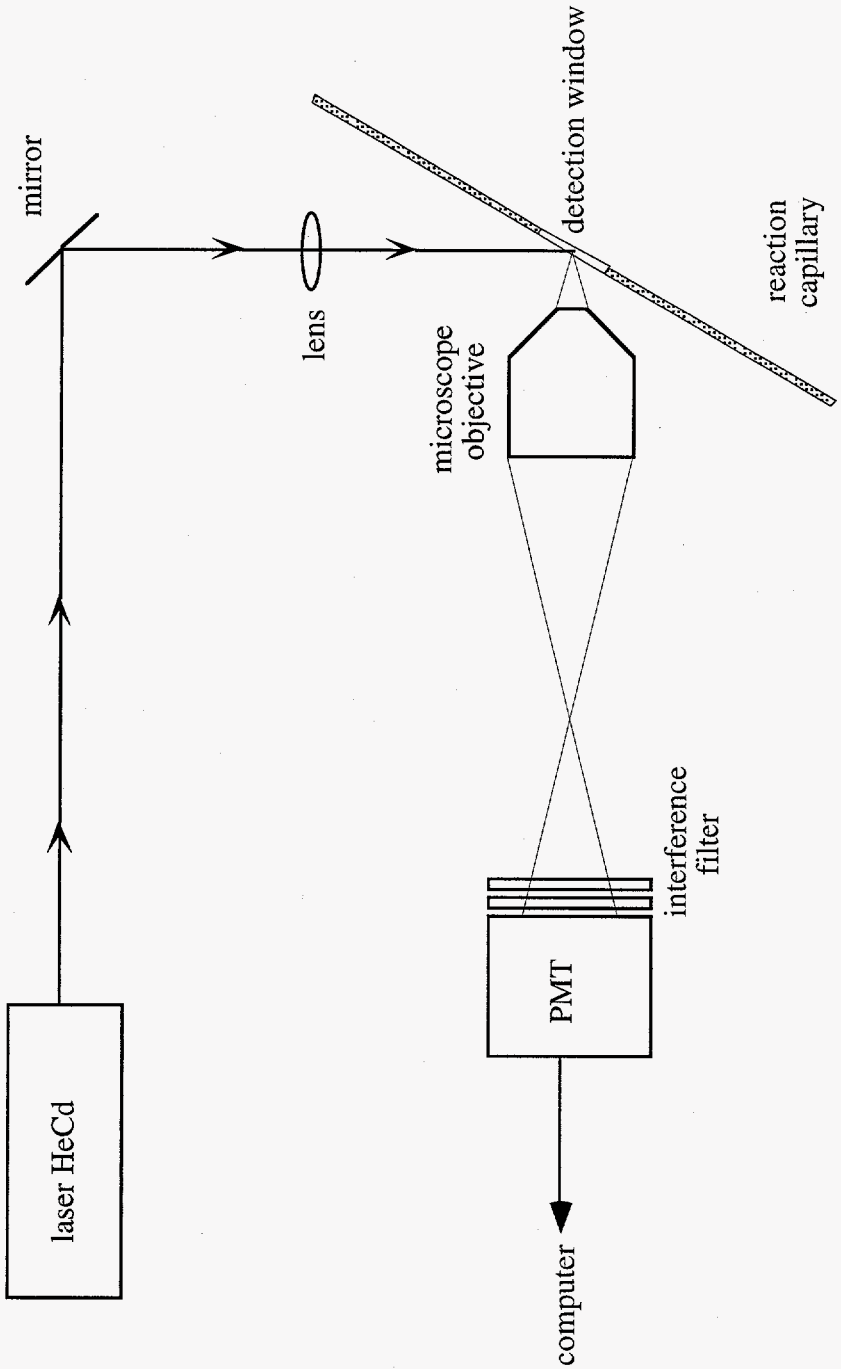

Figure 7. Optical Arrangement for the LIF Detection.

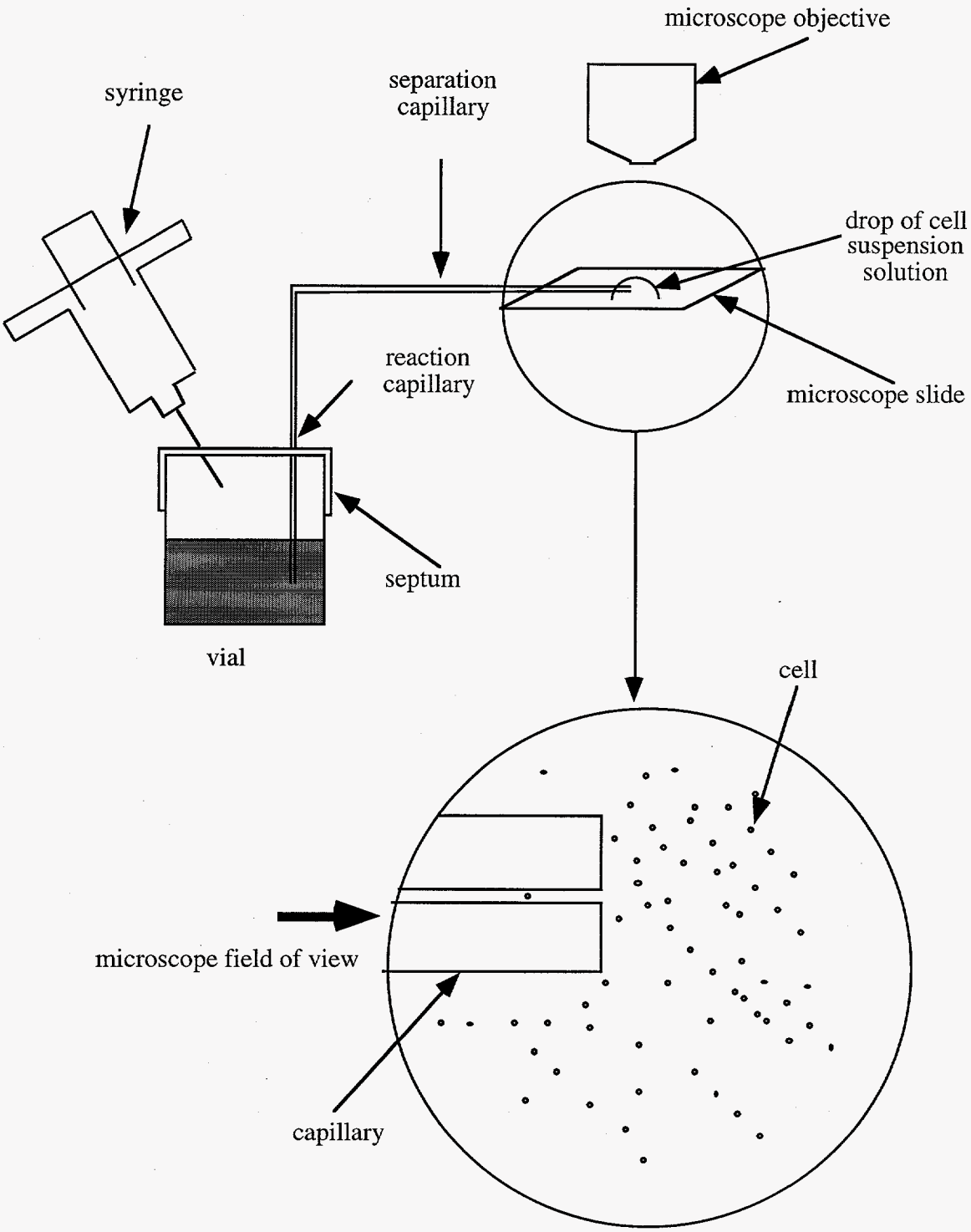

Figure 8. Single Cell Injection.

Results and Discussion

Effect of Voltage Combination on Separation Efficiency. In a coaxial post-column reactor, analyte zones emerging from the separation capillary tip mix with the reagent by means of diffusion, convection and migration [23]. Although thorough mixing is a key for a maximum yield of fluorescent derivatives, turbulent mixing itself broadens analyte zones. Since the electric field strength applied to the separation capillary here is independent of that applied to the reaction capillary, minimum band broadening due to mixing can be achieved by using the appropriate combination of voltages. A series of measurements were carried out using fluorescein as a test compound and borate buffer as the "reagent". The electric field strength across the reaction capillary was kept at 80 V/cm, while different electric field strengths were applied to the separation capillary. Figure 9 shows a plot of the theoretical plate number versus the field strength applied to the separation capillary. The theoretical plate number normally increases as a consequence of increased field strength in the separation capillary since efficiency is directly proportional to the applied voltage in CE [37]. However, axial diffusion is not the limiting factor here. Fig.9 depicts the influence of various degrees of turbulent mixing due to unequial linear velocities between the two inlet streams. The abrupt degradation in efficiency when the field strength for the separation capillary exceeds 154 V/cm suggests the onset of excessive turbulence.

It is interesting to note that the optimum field strength applied to the separation capillary is different from that of the reaction capillary, resulting in unequal linear flow velocities in the two sections. This is likely due to a combination of non-uniform geometry [32], restricted flow from the reagent reservoir, unequal ionic strengths in the two capillary sections, and unequal surface charge (electroosmotic flow coefficient) at the two capillary surfaces. This implies that optimization is needed for each junction if maximum efficiency is required.

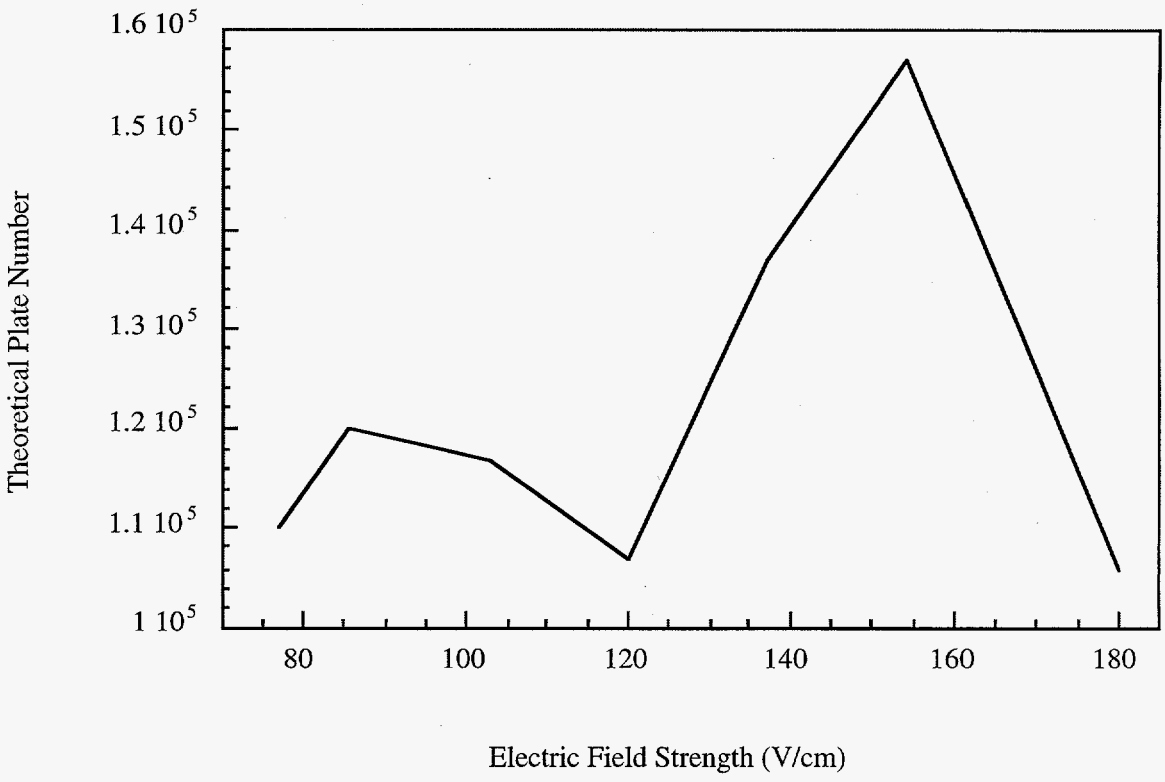

Figure 9. Plot of Theoretical Plate Number As A Function of Applied Electric Field Strength to Separation Capillary When Electric Field Strength Applied to the Reaction Capillary Was Kept At 80 V/cm. Separation Capillary: 50-μm i.d., 32 cm Long; Reaction Capillary: 150-μ m i.d., 12 cm Long.

The relative and absolute electric field strengths also affect the signal size for post-column derivatization. This is because adequate mixing and reaction time are necessary for derivatization. In our case, the peak areas did not vary significantly over the range of voltage combinations used. The peak heights thus increase as the separation efficiency increases. So, fortuitously, Fig.9 also serves to optimize the signal-to-noise ratio.

Linearity and Limits of Detection. From 1 x 10^{-7} to 5 x 10^{-5} M of glycine, the reactor showed a linear response with a slope of 1.09 from a log-log plot of peak area vs. molar concentration. For 2 x 10^{-7} to 2 x 10^{-9} M of human hemoglobin A_0, the slope is 0.971. Fig. 10 shows an electropherogram of 3 x 10^{-8} M human carbonic anhydrase I with a peak efficiency of 190,000. The peak corresponds to 30 attomole of carbonic anhydrase I injected and a 3.8 attomole mass limit of detection, estimated by the criterion of three times the RMS noise.

Limits of detection (S/N = 3) of some biologically important compounds are summarized in Table 1. All compounds were tested with reactors made from 15 μm i. d. x150 μm o. d. and 30 μm id. x 360 μm odd. capillaries.

When compared with the best concentration limits of detection reported in Ref. 16, metanephrine and norepinephrine show lower limits of detection with the post-column reactor, while serotonin, dopamine, and dopa have better limits of detection with the laser induced native fluorescence scheme. Differences in concentration limits of detection between these two methods do not exceed 2.3 times, except that for serotonin which is 85 times worse with the post-column reactor. This highlights the inherent limit of derivatization reactions at low analyte concentrations. Mass limits of detection for all tested amines fall into the low attomole range. For glycine, the best reported mass limit of detection is 130 attomole from an open gap reactor constructed with 10 μm i.d. capillaries [27], while the best reported concentration limit of detection is 1.4 x 10^{-7} M from a

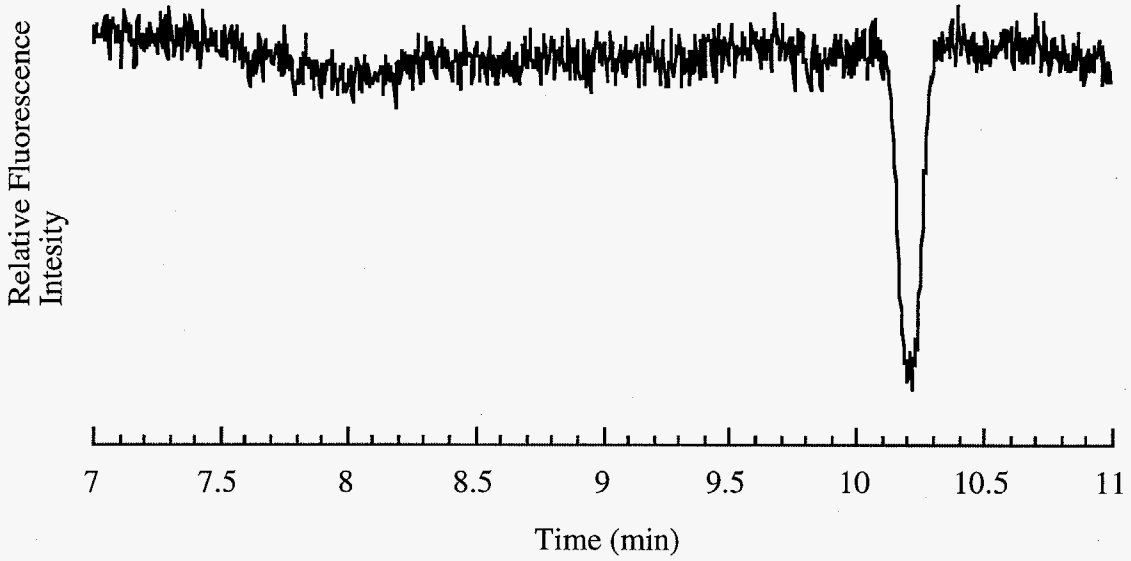

Figure 10. Electropherogram of Human Carbonic Anhydrase I. Peak Corresponds to 30 Attomole Carbonic Anhydrase I Injected. Separation Capillary: 15-μ m i. d., 70 cm long; Reaction Capillary: 30-μm i.d., 12 cm long. Electric Field Strength: 300 V/cm and 150 V/cm for Separation and Reaction Capillaries, Respectively. Injection: 5 s at Operating Voltages.

Table 1.

Detection limits (S/N = 3)of amines, amino acids, proteins and peptides derivatized by OPA/ 2-Mercaptoethanol with LIF detection.

	Concentration Limit of Detection (10^{-8}M)	Mass Limit of Detection (attomole)
Amines		
serotonin	11	153
metanephrine	2.2	23
dopamine	3.7	38
norepinephrine	2.3	20
dopa	18	100
Amino Acids		
glycine	2.7	17
arginine	2.6	32
tryptophan	3.9	35
phenylalanine	10	84
threonine	3.5	26
serine	2.2	17
Proteins		
human hemoglobin A_0	1.1	9.7
human carbonic anhydrase I	0.38	3.8
Peptides		
glutathione	24	310
leucine enkephalin	600	4400
β-casomorphin fragment (1-5)	890	6700
gly-gly-phe-met	720	5700
gly-gly-phe-leu	1300	10000

coaxial reactor [23]. Values in table 1 for glycine show 7.6 times and 5.2 times improvement in mass and concentration limits of detection, respectively. Mass limits of detection for tested amino acids are fairly close to each other, i.e. in the low attomole range.

OPA/2-ME has been known as a good fluorogenic reagent for proteins [39,40]. Mass limits of detection for human hemoglobin A_0 and carbonic anhydrase I are better than those for amines and amino acids. A 9.7 attomole mass limits of detection for hemoglobin A_0 is similar to that obtained from the laser induced native fluorescence [15], and is sufficient for hemoglobin assay in individual human erythrocytes.

OPA/2-ME labeled peptides have been found to have low fluorescence quantum yields [33]. Although mass limits of detection for peptides are poor compared with those for proteins, they still fall in low femtomole range with an exception for glutathione which is 310 attomoles.

Single Cell Capability Demonstration. Fig.11 depicts a set of electropherograms from single human erythrocyte experiments plotted on a common scale. The blood sample was from a finger tip of a healthy human female adult. Between consecutive cell injections, capillaries were pressure flushed for 5 minutes with the borate buffer followed by a 3 minute re-equilibration under operating voltages. This treatment turned out to be crucial because the efficiency and sensitivity were greatly degraded after one run. Fortunately, this cleaning procedure was effective enough to regain good performance.

The common features in these electropherograms are peak A and peak B. By spiking a hemolysate of the same blood sample, peak A was identified as hemoglobin, the most abundant protein in erythrocytes (existing at about 450 attomole per human erythrocyte[41]), and peak B was identified as carbonic anhydrase I. Detailed discussion on hemoglobin quantity variation along with the migration time variation from cell to cell can be found in Ref. 15. At the first glimpse,

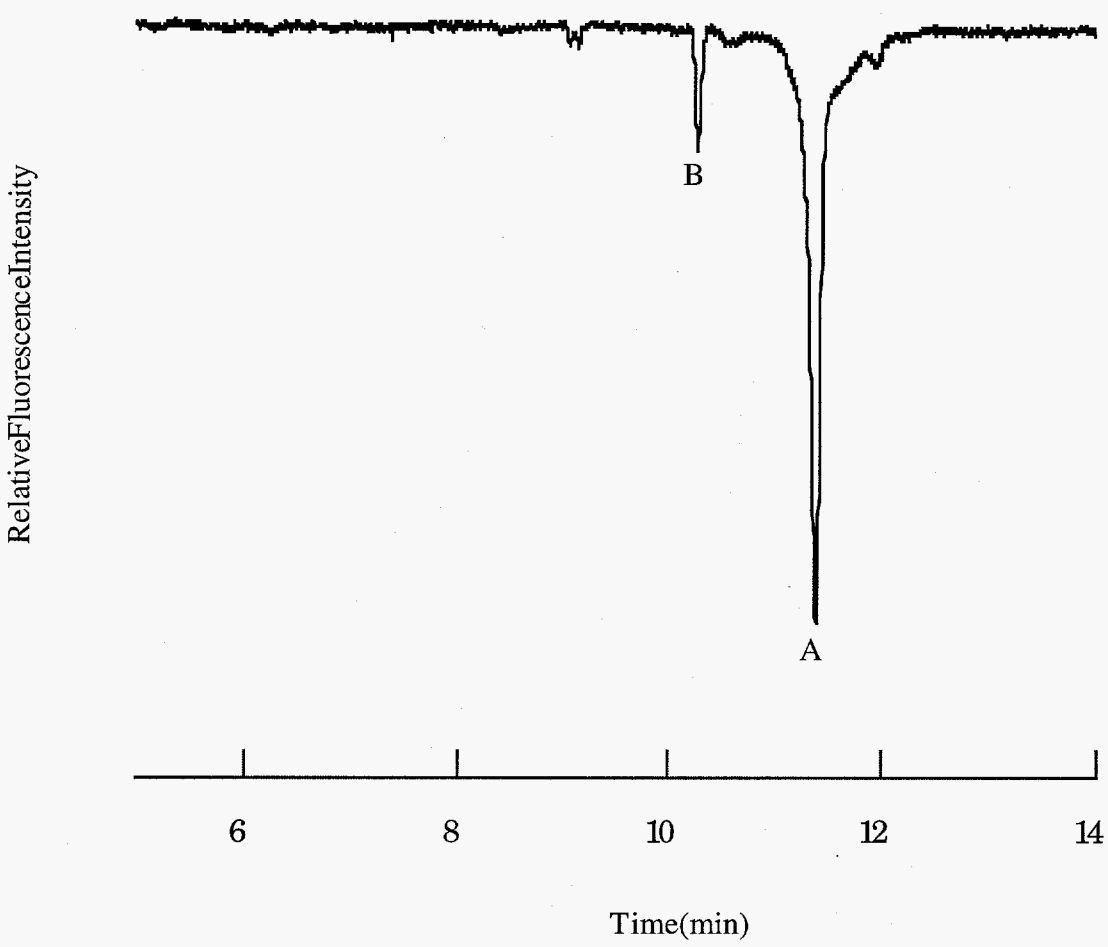

Figure 11. Eletropherograms of Single Normal Erythrocytes. Separation Capillary: 15-μ m i. d., 70 cm Long; Reaction Capillary: 30-μm i.d., 12 cm Long. Electric Field Strength: 300 V/cm and 150 V/cm for Separation and Reaction Capillaries, Respectively. Injection: See Text.

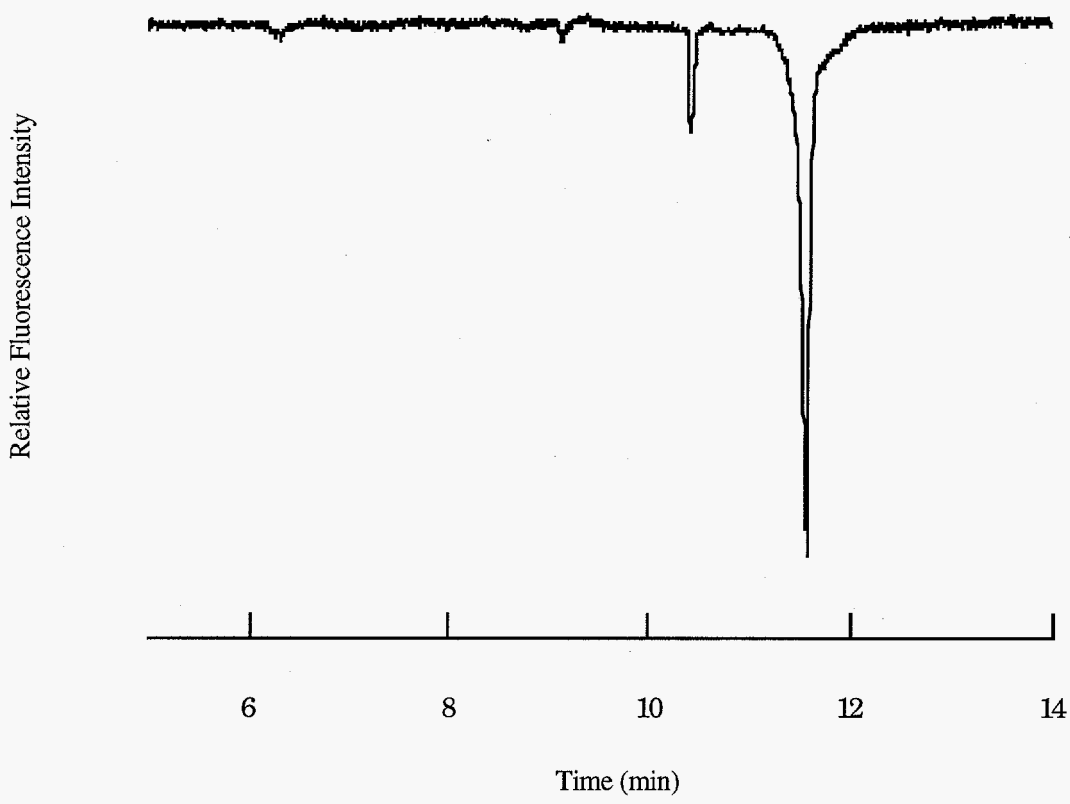

Figure 11. (continued)

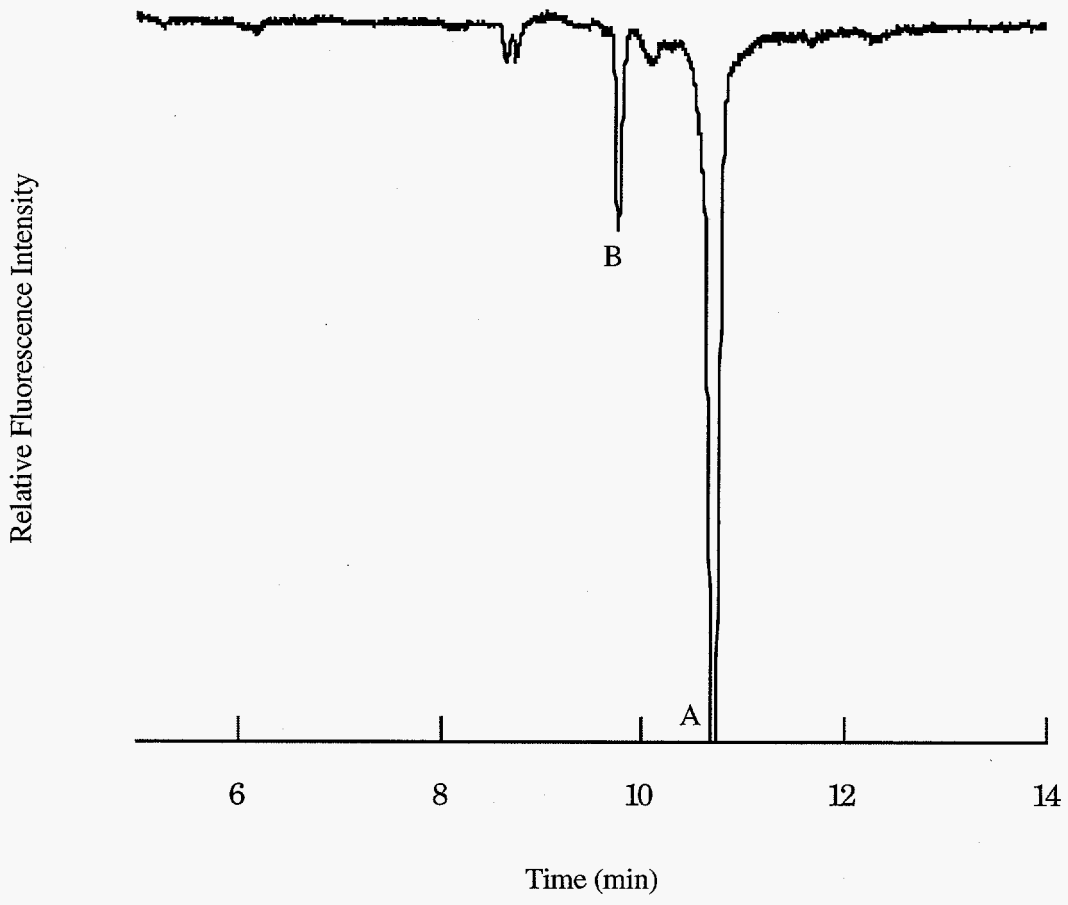

Figure 11. (continued)

carbonic anhydrase I, contained in human erythrocytes at a mean level of about 10 attomole per erythrocyte [42], should not give a peak of the size shown in these electopherograms based on 3.8 attomole limit of detection for human carbonic anhydrase I. The concentration of carbonic anhydrase, however, varies significantly from race to race [43,44], person to person [46] and also from cell to cell [15]. Other less prominent peaks are believed to be from less abundant primary amine group containing species in erythrocytes.

Fig.12 is a set of electropherograms of single human erythrocyte experiments with a blood sample from an adult diabetic patient. Again, they are plotted on a common scale. Compared with fig. 5, this set of electropherograms shows a very different diabetic erythrocyte composition from that of normal erythrocytes. The fact that this composition difference is not detected by laser induced native fluorescence [46] indicates the post-column derivatization reactor opens up a new way to assay non-fluorescent components in individual cells.

Fig.13 depicts a set of electropherograms of single cell experiments with a human fetal blood sample. An early survey concluded that the mean concentration of carbonic anhydrase I (the main carbonic anhydrase isozyme found in human erythrocytes acounting for 83% of total carbonic anhydrase concentration [36]) in one-year-children reaches only about 40% of the mean concentration of normal adults [40]. The absence of peak B in these electropherograms, showing that the concentration of carbonic anhydrase I in fetal erythrocytes is much lower than that in adults, is in good agreement with the early findings.

In summary, a new post-column reactor for CE has been developed. Low attomole range mass limits of detection provided by this postcolumn reactor facilitate sensitive detection of a variety of biologically important amines, amino acids and proteins simultaneously with a single optical arrangement and a relatively inexpensive laser. Single cell capability demonstrated here shows that this reactor could find applications in assaying non-fluorescent or electrochemically inactive components in individual biological cells in the future.

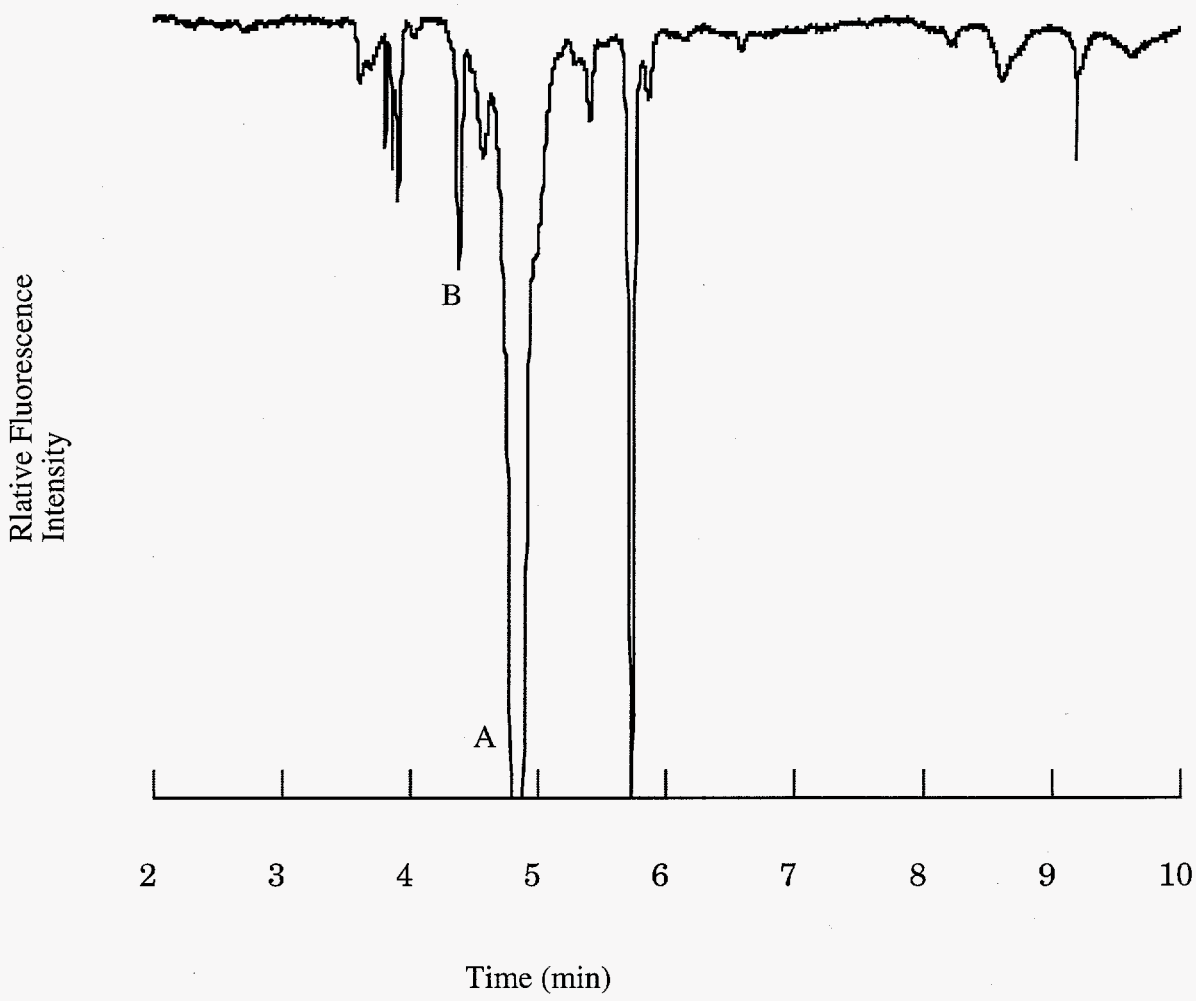

Figure 12. Eletropherograms of Single Diabetic Erythrocytes. Separation Capillary: 15-μ m i. d., 32 cm Long; Reaction Capillary: 30-μm i.d., 12 cm Long. Electric Field Strength: 300 V/cm and 150 V/cm for Separation and Reaction Capillaries, Respectively. Injection: See Text.

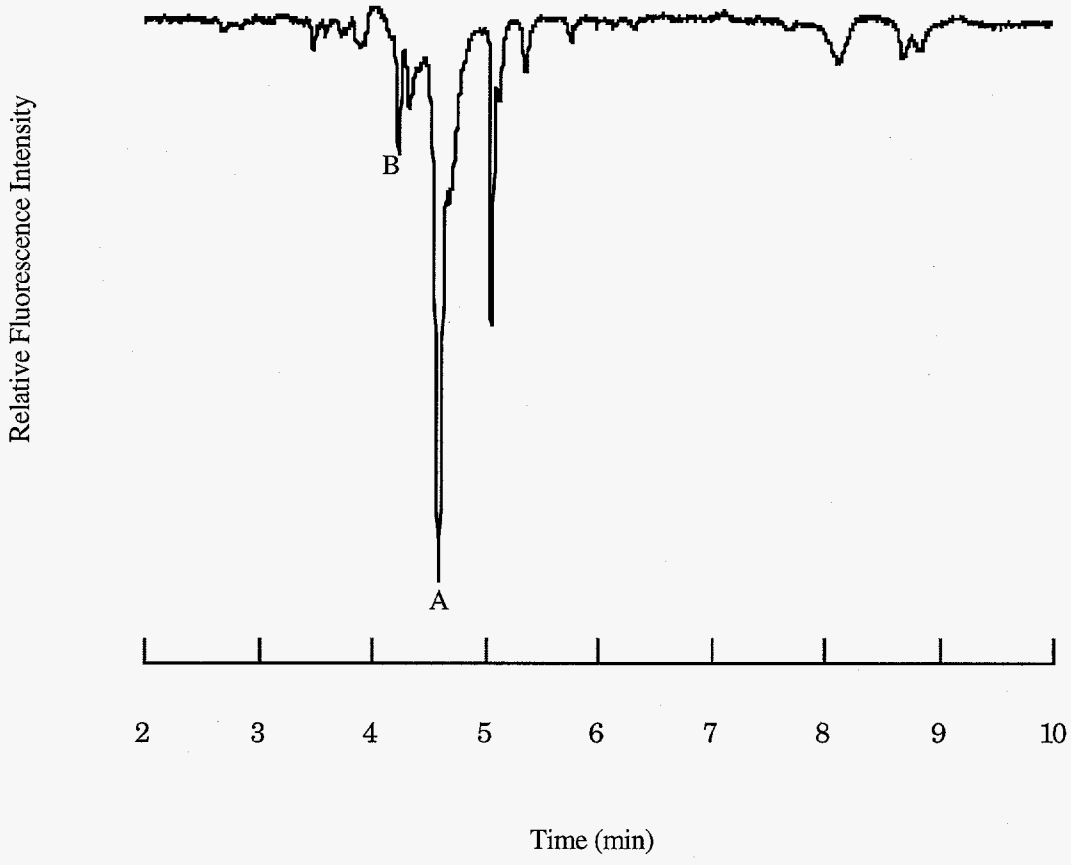

Figure 12. (continued)

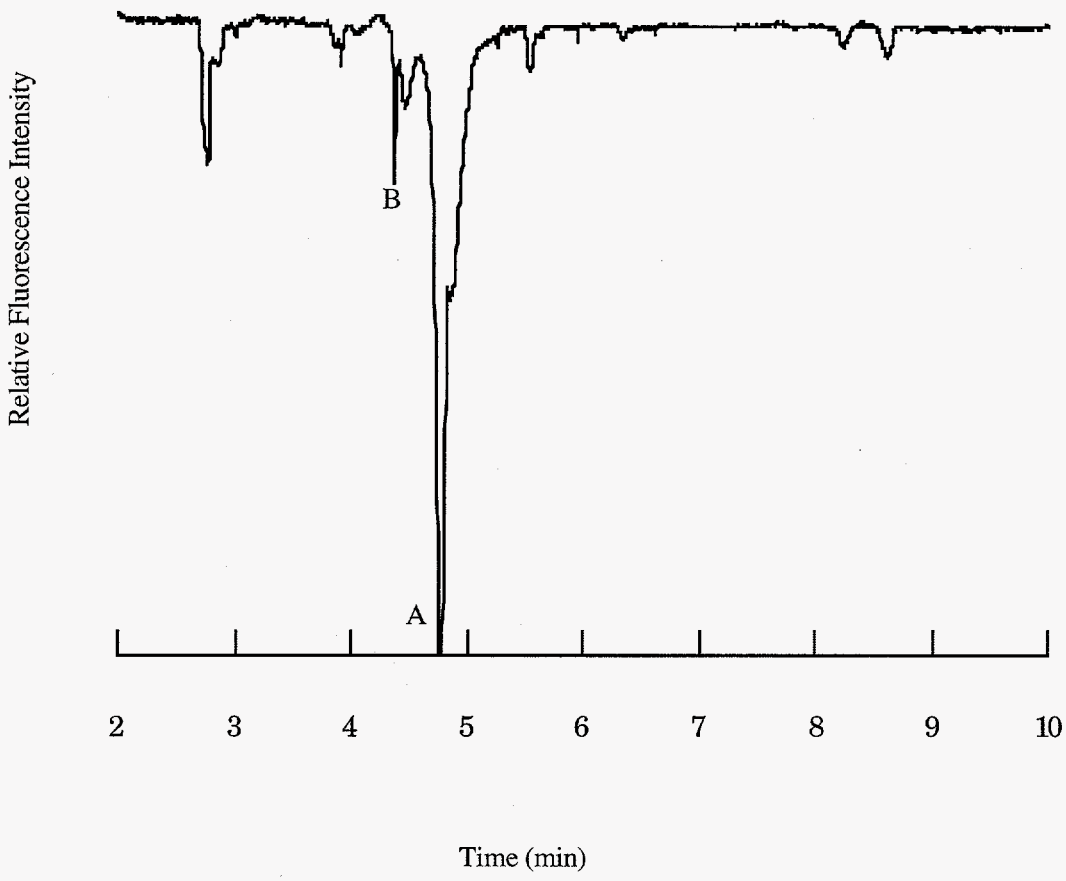

Figure 12. (continued)

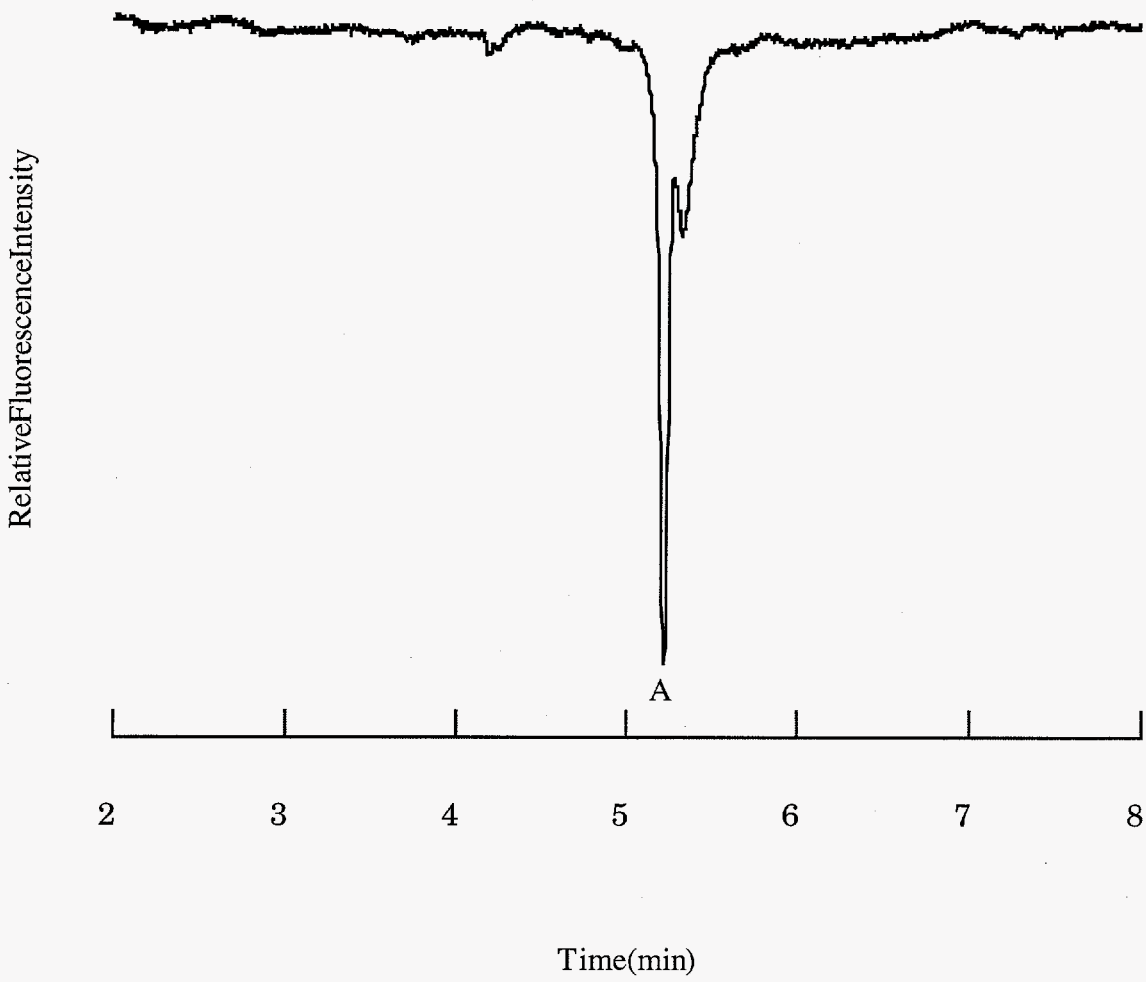

Figure 13. Eletropherograms of Single Fetal Erythrocytes. Same Conditions as in Figure 12.

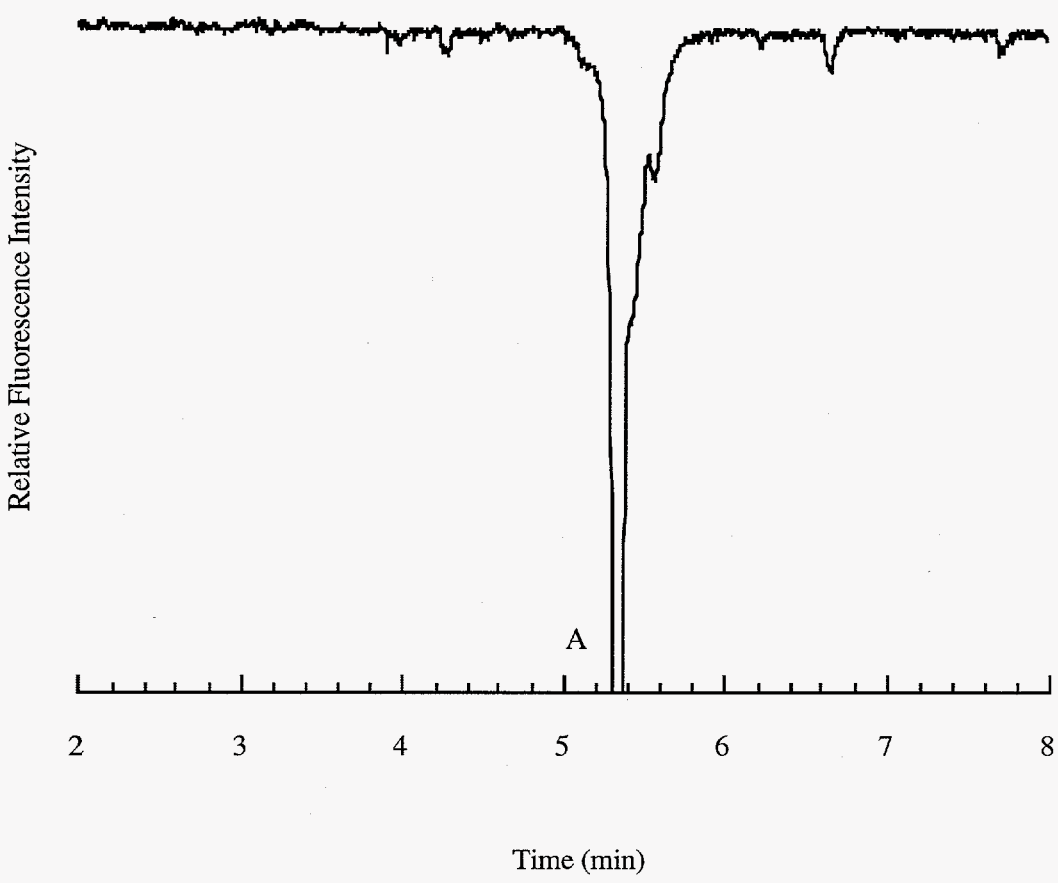

Figure 13. (continued)

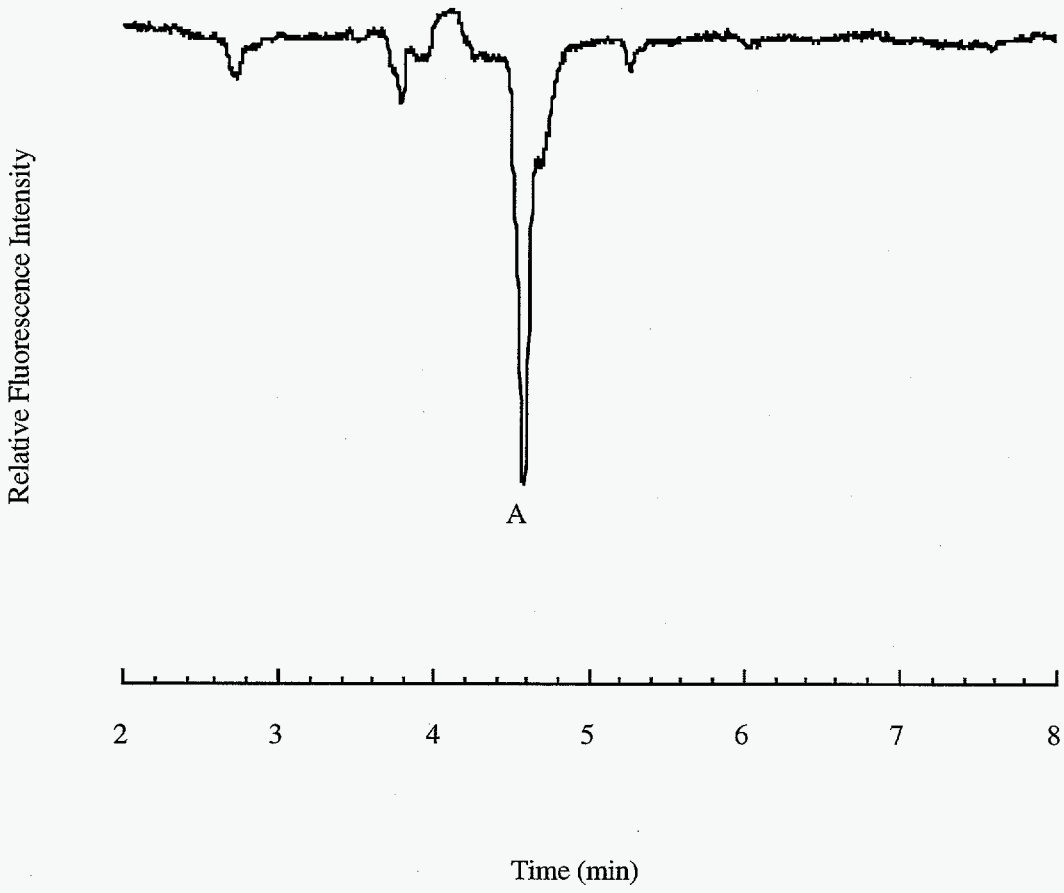

Figure 13. (continued)

REFERENCES

1. W.R. Jones and P. Jandik, J. Chromatogr., 546 (1991) 445.
2. A. Weston, P.R. Brown, P. Jandik, W.R. Jones and A.L. Heckenberg, J. Chromatogr., 593 (1992) 259.
3. F-T.A. Chen, and J.C. Sternberg, Electrophoresis, 15 (1994) 13.
4. S. Molton, H. Frischknecht and W. Thormann, Electrophoresis, 15 (1994) 22.
5. E.N. Fung and E.S. Yeung, Anal. Chem., 67 (1995) 1913.
6. Reinhard Kuhn and Sabrina Hoffstetter-Kuhn, Capillary Electrophoresis: Principles and Practice, Springer-Verlag. Berlin, Heidelberg, New york, London, Paris, Tokyo, Hong Kong, Bercelona, Budapest. 1993.
7. S. Hjerten. J Chromatogr. 347 (1985) 189.
8. J. Liu, V. Dolink, Y.-Z. Hsieh and M. Novotny, Anal. Chem. 64 (1992) 1328.
9. E.S. Yeung, Adv. Chromatogr., 35 (1995) 1.
10. A.G. Ewing, J.M. Mesaros and P.F. Gavin, Anal. Chem., 66 (1994) 527A.
11. A. Nann and E. Pretsch, J. Chromatogr. A, 676 (1994) 437.
12. S.A. Hofstadler, F.D. Swanek, D.C. Gale, A.G. Ewing and R. D. Smith, Anal. Chem., 67 (1995) 1477.
13. S. Wu and N.J. Dovichi, J. Chromatogr., 480 (1989) 141.
14. T.T. Lee and E.S. Yeung, J. Chromatogr., 595 (1992) 319.
15. T.T. Lee and E.S.Yeung, Anal. Chem., 64 (1992) 3045.
16. H-T. Chang and E.S. Yeung, Anal Chem., 67 (1995) 1079.
17. B. Nickerson and J.W. Jorgenson, J. Chromatogr., 480 (1989) 157.

18. C.P. Ong, C.L. Ng, H.K. Lee and S.F.Y. Li, J. Chromatogr., 559 (1991) 537.

19. M.D. Oates, B.r. Cooper and J.W. Jorgenson. Anal. Chem. 62 (1990) 1573.

20. S.D. Gilman and A.G. Ewing, Anal. Chem. 67 (1995) 58.

21. N.J. Reinhold, U.R. Tjaden J.V.D. Greef, J. Chromatogr., 673 (1994) 255.

22. B. Nickerson and J.W. Jorgenson, J. Chromatogr., 480 (1989) 157.23.D.J. Rose, Jr. and J.W. Jorgenson, J. Chromatogr., 447 (1988) 117.

24. A. Emmer and J. Roeraade, J. Chromatogr. A, 662 (1994) 375.

25. S.L. Pentoney, Jr., X. Huang, D.S. Burgi and R.N. Zare, Anal. Chem., 60 (1988) 2625.

26. M. Albin, R. Weinberger, E. Sapp and S. Morning, Anal. Chem., 63 (1991) 417.

27. S.D. Gilman, J.J. Pietron and A.G. Ewing, J. Microcol. Sep., 6 (1994) 373.

28. S.C. Jacobson, L.B. Koutny, R. Hergenroder, A.W. Moore, Jr. and J.M. Ramsey. Anal. Chem., 66 (1994) 3472.

29. M. Roth, Anal. Chem., 43 (1971) 880.

30. S.S. Simons, Jr., and D.F. Johnson, J. Am. Chem. Soc., 98 (1976) 7098.

31. C. Buteau, C. L. Duitschaever and G. C. Hshton, J. Chromatogr., 212 (1981) 23.

32. S.S. Simons, Jr., and D.F. Johnson, Anal. Biochem., 82 (1977) 250.

33. R.F. Chen, C. Scott, and E. Trepman, Biochim. Biophys. Acta, 576 (1979) 440.

34. R.C. Simpson, H.Y. Mohammed and H. Veening, J. Liq. Chromatogr. 5 (1982) 245.

35. R. Kucera and H Umagat, J. Chromatogr. 255 (1983) 563.

36. J.A. Jankowski, S. Tracht and J.V. Sweedler, Trends in Anal. Chem., 14 (1995) 170.

37. J.W. Jorgenson and K.D. Lukacs, Anal. Chem., 53 (1981) 1298.

38. Y. Xue and E. S. Yeung, Anal. Chem., 66 (1994) 3575.

39. E. Weidekamm, D.F.H. Wallach and R. Fluckiger, Anal. Biochem., 54 (1973) 102.

40. H. Kutchai and L.M. Geddis, Anal. Biochem., 77 (1977) 315.

41. R.B. Pennell, in The Red Blood Cell, 2nd ed.; D.M.-N. Surgenor Ed;

42. N.D. Carter, R. Heath, R.J. Welty, D. Hewett-Emmett, S. Jeffery, A. Shiels and R.E. Tashian, Ann. NY. Acad. Sci., 429 (1984) 284.

43. K. Goriki, R. Hazama, and M. Yamakido, Ann. NY. Acad. Sci., 429 (1984) 276.

44. M.J. Moore, Ann. NY. Acad. Sci., 429 (1984) 277.

45. J.N. Shepherd and N. Spencer, Ann. NY. Acad. Sci., 429 (1984) 280.

46. S.J. Lillard, E.S. Yeung, R.M.A. Lautamo and D.T. Mao, J. chromatogr., in press.

Acknowledgments

This work was performed at Ames Laboratory under Contract No. W-7405-Eng-82 with the U.S. Department of Energy. The United States government has assigned the DOE report number IS-T 1770 to this thesis